Anomalous local spin susceptibilities in noncentrosymmetric La_2C_3 superconductor

Anton Potočnik and Peter Jeglič
Jožef Stefan Institute, Jamova c. 39, SI-1000 Ljubljana, Slovenia

Kaya Kobayashi, Kenji Kawashima, Saori Kuchida, and Jun Akimitsu
Aoyama Gakuin University, 5-10-1 Fuchinobe Sagamihara 252-5258, Japan

Denis Arčon*
Jožef Stefan Institute, Jamova c. 39, SI-1000 Ljubljana, Slovenia
and Faculty of Mathematics and Physics, University of Ljubljana, Jadranska c. 19, SI-1000 Ljubljana, Slovenia
(Received 8 July 2014; revised manuscript received 31 August 2014; published 11 September 2014)

We report on ^{139}La and ^{13}C nuclear magnetic resonance (NMR) study of noncentrosymmetric superconductor La_2C_3 with superconducting critical temperature $T_c = 11.8$ K. In the normal state ^{139}La NMR spectra show a characteristic quadrupole polycrystalline broadening yielding a quadrupole frequency $\nu_Q = 3.1$ MHz and a very large shift of ∼3000 ppm. A significant part of this shift arises from the Van Vleck-like susceptibility as a result of a sizable spin-orbit coupling. In the superconducting phase La_2C_3 shows abnormal behavior that dramatically deviates from the conventional *s*-wave superconductors. Namely, (i) ^{139}La and ^{13}C NMR shifts in the superconducting state do not change from their normal-state values, and (ii) the ^{139}La spin-lattice relaxation rate is strongly enhanced below T_c. Such unconventional response in the local static and dynamic spin susceptibilities is discussed in terms of possible mixture of spin-singlet and spin-triplet Cooper pairs, which is promoted by the asymmetric spin-orbit coupling in the system without the center of inversion.

DOI: 10.1103/PhysRevB.90.104507 PACS number(s): 74.70.Wz, 74.20.Rp, 74.25.nj

I. INTRODUCTION

Light element molecular solids with s/p-based outer electrons in which a fine balance exists between electron-phonon coupling and electron correlation energies can give rise to some most intriguing electronic properties usually associated only with the transition-metal ions. For example, orbital ordering and unconventional magnetism have been reported for correlated alkali-metal sesquioxides and superoxides [1,2] while high-temperature superconductivity has been found in expanded fullerides [3,4]. Rare-earth sesquicarbides (Ln_2C_3, Ln = La, Y) with characteristic C_2 dumbbell molecular units fall into the same category of materials as relatively high superconducting critical temperatures up to T_c∼ 18 K [5] arise from the light atomic mass of carbon.

Ln_2C_3 crystallize in the body center cubic (bcc) Pu_2C_3 structure [space group $I\bar{4}3d$, Fig. 1(a)] [6]. This space group lacks the inversion symmetry. Therefore, the parity constrain, which in the superconducting state selects between spin-singlet or spin-triplet states of the Cooper pairs, is broken [7]. Moreover, in systems without inversion symmetry the asymmetric spin-orbit interaction is allowed thus providing a microscopic mechanism for a mixing of spin-singlet and spin-triplet pairings [7,8]. This has been indeed observed in certain heavy-fermion compounds [9–14], but the results for Ln_2C_3 are far less conclusive. Recent magnetic penetration depth and upper critical field measurements on Y_2C_3 yielded evidences of nodal superconducting gap structure [15], which were attributed to the mixed spin-singlet and spin-triplet pairing states within the same orbital channel. On the other hand, although the spin-orbit interaction is expected to be even stronger in isostructural La_2C_3 compared to related Y_2C_3, specific-heat and upper critical field measurements on former compound suggested a single superconducting gap with *s*-wave symmetry in the strong electron-phonon coupling limit [16]. A different conclusion was derived from muon-spin relaxation [17] and ^{13}C spin-lattice relaxation time [18] measurements, which were consistent with a multigap superconductivity that opens the possibility for the coupling to different phonon modes and complex superconducting order parameters and could account for the relatively high $T_c \approx 18$ K [5] in Ln_2C_3 compounds.

Sample quality is very important in Ln_2C_3. For example, in different La_2C_3 samples the reported T_c values vary between 5.6–13.4 K [17,19–21]. Such pronounced spread of the critical temperatures has been ascribed to the variations in the precise carbon stoichiometry where the highest T_c was claimed in the perfectly stoichiometric samples [20]. Therefore, some of the ambiguities in describing the superconducting state of Ln_2C_3 may arise also from the difficulties in the sample preparation. Studies of high-quality samples are thus required to address the impact of noncentrosymmetric structure in these compounds.

Stimulated by such conflicting results for the Ln_2C_3 family we decided to investigate the superconducting pairing symmetries in La_2C_3 by employing ^{139}La and ^{13}C nuclear magnetic resonance (NMR) technique in order to probe the local static and dynamic spin susceptibilities in the normal and in the superconducting state [22]. Surprisingly, we found that the ^{139}La Knight shift is large and nearly the same in the normal and superconducting states while the spin-lattice relaxation rate becomes even enhanced below T_c in striking contrast to what is anticipated for the conventional spin-singlet pairing states. Both anomalous dependences are compatible with the mixing of spin-singlet and spin-triplet Cooper pairs in the studied high-quality La_2C_3 sample.

*denis.arcon@ijs.si

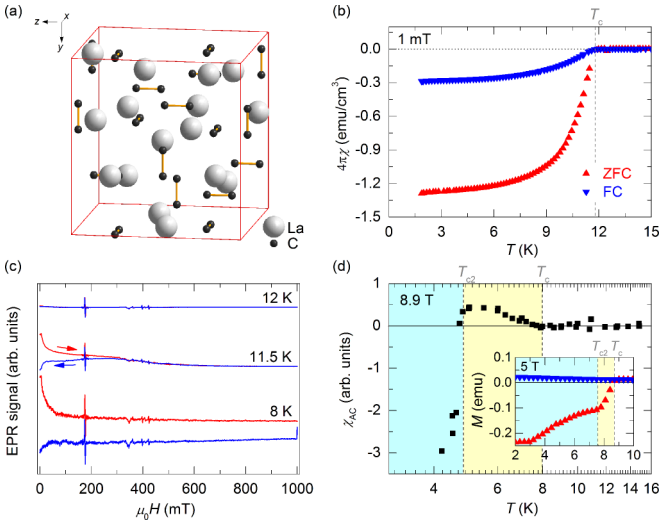

FIG. 1. (Color online) (a) Crystal structure of La_2C_3 superconductor where large gray spheres indicate the positions of La atoms while smaller black spheres stand for the carbon atoms that form C_2 dumbbells. C-C bonds are represented by thick orange line. (b) Temperature dependence of dc magnetic susceptibility, χ, measured during the zero-field cooling (ZFC, red up triangles) and field-cooling (FC, blue down triangles) temperature protocols at 1 mT. Dashed vertical line marks $T_c = 11.8(2)$ K. (c) Magnetically modulated microwave absorption signal measured at 9.7 GHz for up (red) and down (blue) magnetic field sweep directions. Sharp resonance at ∼170 mT and several weaker ones between 320 and 430 mT are spurious EPR signals of the dielectric microwave resonator. (d) Dynamic spin susceptibility, χ_{ac}, measured *in situ* in the NMR circuit as a shift of the resonant frequency at a magnetic field of 8.9 T. Dashed vertical lines at $T_c = 8.0(5)$ K and $T_{c2} = 4.8(2)$ K mark two superconducting transitions in the magnetic field of 8.9 T. Inset: Static magnetization measurement (red up triangles stand for ZFC while blue down triangles stand for FC measurements) at 5 T where two transitions can be observed at $T_c = 8.7(1)$ K and $T_{c2} = 7.5(1)$ K.

II. METHODS

A. Material preparation and characterization

The La_2C_3 polycrystalline sample was prepared by the standard arc melting method using a mixture of La (99.9%) and C (graphite, 99.99%) with stoichiometric composition of sesquicarbide following the same procedure as in Ref. [17]. The obtained La-C alloy was pressed into pellets in a sealed tantalum tube and sintered at 1000 °C for 200 h under a high vacuum condition of 3.0×10^{-5} Torr, followed by a slow cooling back to ambient temperature at a rate of 5 °C/h.

The powder x-ray diffraction pattern was indexed as La_2C_3 sesquicarbide phase with the space group of $I\bar{4}3d$. The room-temperature lattice constant was determined to be $a = 8.808(5)$Å, which is in good agreement with those reported previously [6,16,19]. The precise stoichiometry of carbon has not been determined. Therefore, the chemical composition in this article refers only to its nominal value. Close inspection of x-ray diffraction pattern also reveals ∼0.28% of LaC_2 as a minor impurity phase.

Static (dc) magnetic susceptibilities, χ, were measured between 2–300 K in fields up to 7 T using the standard MPMS apparatus (Quantum Design Co., Ltd.).

B. Magnetically modulated microwave absorption

Magnetically modulated microwave absorption (MMMA) was measured on a commercial Bruker E580 X-band (9.7 GHz) electron paramagnetic resonance (EPR) spectrometer using an Oxford cryogenics continuous flow cryostat. The temperature stability was better than ±0.1 K over the entire temperature range. The hysteresis of the microwave absorption signal [23,24] was measured first by sweeping the magnetic field up from 0 to 1 T and then in the second step by sweeping back from 1 T to 0. In both cases the sweeping rate was 11.9 mT/s. For all measurements the microwave power was 2 mW, the magnetic modulation frequency 100 kHz and the modulation amplitude 0.2 mT. For each MMMA measurement at a given temperature the sample was first heated to a temperature above T_c and then cooled down to the desired temperature in the zero magnetic field.

C. NMR measurements

^{139}La (nuclear spin $I = 7/2$) NMR spectra and the spin-lattice relaxation time, T_1, were measured between 4.9 and 300 K in two different magnetic fields of 8.9 T and 4.7 T, respectively. All ^{139}La NMR shifts are determined relative to the Larmor frequencies $\nu_L(^{139}\text{La}) = 53.6810$ MHz (8.9 T) and 28.2520 MHz (4.7 T), which were defined by measuring 0.01 M $LaCl_3$ in H_2O standard. For ^{139}La NMR line shape measurements a Hahn-echo pulse sequence, $\pi/2 - \tau - \pi - \tau -$ echo, was used, with a pulse length $t_w(\pi/2) = 2.5\,\mu$s and an interpulse delay $\tau = 20\,\mu$s. The complete polycrystalline NMR spectrum was obtained by summing the real part of spectra measured at different frequencies separated by $\Delta\nu = 50$ kHz.

Details of ^{139}La NMR spectra simulations, which included the hyperfine coupling interaction and corrections of the quadrupole interaction up to the second order, are provided in the Appendix. For the fitting of the ^{139}La NMR central transition line [Fig. 2(b)] we considered only homogeneous broadening, i.e., no broadening due to the anisotropic shift tensor or the distribution of quadrupole splitting frequency, ν_Q, was required. However, simulations of the entire polycrystalline spectrum comprising of central and satellite transitions [blue line in Fig. 2(a)] reveal a small distribution of ν_Q at 80 K. We note that for simplicity reasons the NMR shift tensor was assumed to be isotropic for all spectral analysis. ^{139}La NMR line shape fitting allowed for the determination of the quadrupole splitting frequency [25] $\nu_Q = \frac{3eV_{zz}Q}{h2I(2I-1)}$ and the asymmetry parameter $\eta = (V_{xx} - V_{yy})/V_{zz}$ defined by the components of electric field tensor (EFG) tensor (V_{ij}). Here Q is the quadrupole moment of ^{139}La and h is the Planck's constant.

For T_1 measurements an inversion recovery pulse sequence was employed. T_1 measurements were performed on the high-frequency singularity of the central transition line (specifically, at $\nu = 53.99$ MHz at 8.9 T and $\nu = 28.64$ MHz at 4.7 T) and for this reason the ^{139}La magnetization, $M(\tau)$, recovery curve

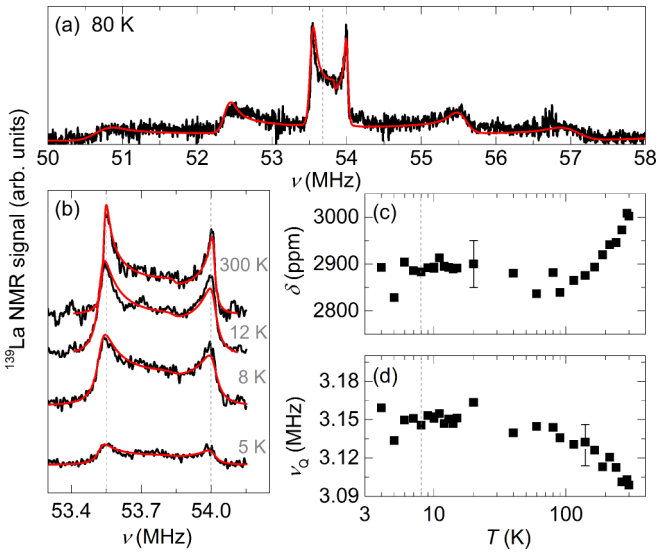

FIG. 2. (Color online) (a) ^{139}La NMR spectrum of polycrystalline La_2C_3 (thick black line) measured at 80 K. Red line is a fit to the model including quadrupole interaction up to the second order (see text for details). Dashed vertical line marks the reference frequency against which all shifts are measured. (b) Central transition lines of the ^{139}La NMR spectra (black lines) at selected temperatures above and below the critical temperature. Note that the signals were multiplied with the temperature to correct their intensity for the Boltzmann factor. Dashed vertical lines indicate positions of the two singularities at 300 K. Temperature dependences of ^{139}La NMR shift, δ, (c) and of quadrupole splitting frequency, ν_Q, (d). Both parameters were extracted from the line shape fits of the central $(-1/2 \leftrightarrow 1/2)$ transition [Fig. 2(b)]. Dashed vertical lines indicate the superconducting critical temperature at 8.9 T.

was fitted by the following expression [26]:

$$M(\tau) = A + B\left(1 - \frac{1}{84}e^{-(\frac{\tau}{T_1})^\alpha} - \frac{3}{44}e^{-(\frac{6\tau}{T_1})^\alpha} - \frac{75}{364}e^{-(\frac{15\tau}{T_1})^\alpha} - \frac{1225}{1716}e^{-(\frac{28\tau}{T_1})^\alpha}\right).$$

Here T_1, stretched exponent α, and amplitudes A, B were free fitting parameters related to the initial and thermal equilibrium ^{139}La nuclear magnetization. Stretched exponent α was found to be nearly temperature independent. In the final analysis for experiment performed in 4.7 T its average value of $\alpha = 0.75$ was thus kept fixed for all temperatures.

^{13}C (nuclear spin $I = 1/2$, natural abundance 1.1%) NMR spectra and the spin-lattice relaxation time, $^{13}T_1$, were measured in the magnetic field of 9.39 T. Reference frequency, $\nu_L(^{13}C) = 100.5699$ MHz, was obtained from the tetramethylsilane (TMS) standard. For ^{13}C NMR line shape measurements a Hahn-echo pulse sequence was used with a pulse length $t_w(\pi/2) = 12\,\mu$s and an interpulse delay $\tau = 50\,\mu$s. For $^{13}T_1$ measurements an inversion recovery Hahn-echo technique was adopted.

III. RESULTS

A. Magnetization measurements

Temperature dependence of static magnetization of the La_2C_3 polycrystalline sample shows a characteristic diamagnetic response below $T_c = 11.8(2)$ K [Fig. 1(b)]. The marked difference between the zero-field-cooled (ZFC) and field-cooled (FC) magnetization below T_c shows the Meissner effect and thus confirms that the observed diamagnetic response is due to the onset of superconductivity. The large superconducting fraction (at 2 K it even exceeds 100% because of the large uncertainty in estimating the effects of the demagnetization factor) complies with the bulk superconducting response. The bulk superconducting state is additionally confirmed by the observation of the low-field MMMA, which originates from the dissipation of microwave energy due to the vortex motion [23,24]. The MMMA signal is clearly detected below $T_c \approx 11.5(5)$ K as a hysteresis of microwave absorption signal at low fields [Fig. 1(c)] that grows with decreasing temperature. We stress that no paramagnetic EPR signal that could originate from paramagnetic centers (impurities) in the sample was detected between room temperature and 4 K.

The near optimal critical temperature of the present sample confirms its high quality—the carbon off stoichiometry thus must be very small. In quantitative agreement with the established magnetic field suppression of T_c for La_2C_3 [20] our magnetization measurements in 5 T magnetic field show that T_c decreases to 8.7(1) K [inset to Fig. 1(d)]. At even higher fields (8.9 T) T_c is further suppressed to $T_c = 8.0(5)$ K [Fig. 1(d)] as concluded from the anomaly in the dynamic susceptibility, χ_{ac}, measured *in situ* in the NMR circuit. However, contrary to expectations for the spin-singlet pairing χ_{ac} actually first increases below T_c before showing the conventional diamagnetic response below $T_{c2} = 4.8(2)$ K. We also note that at 5 T an anomaly is observed in the dc magnetization at $T_{c2} = 7.5(1)$ K while it is absent for magnetic fields lower than 4 T. This behavior cannot be attributed to sample inhomogeneities, since a single well-defined T_c was found in the low-field measurements [Fig. 1(b)]. The superconducting state is thus anomalous for $T_{c2} < T < T_c$ so we proceed to investigate it with ^{139}La NMR measurements.

B. NMR in the normal state

^{139}La $(I = 7/2)$ NMR spectrum measured at 80 K [Fig. 2(a)] is very broad, with detectable intensity spanning over 6 MHz. The central $(-1/2 \leftrightarrow 1/2)$ as well as the satellite $(\pm 7/2 \leftrightarrow \pm 5/2, \pm 5/2 \leftrightarrow \pm 3/2, \pm 3/2 \leftrightarrow \pm 1/2)$ transitions can be clearly identified, which imply that the polycrystalline broadening is primarily due to the strong quadrupole interaction. We thus analyze polycrystalline ^{139}La NMR spectra (Fig. 2) with the general spin Hamiltonian $\mathcal{H} = \mathcal{H}_Z + \mathcal{H}_Q + \mathcal{H}_S$ that is comprised of nuclear Zeeman ($\mathcal{H}_Z$) and quadrupole ($\mathcal{H}_Q$) terms as the strongest interactions. $\mathcal{H}_S$ gives rise to the shift of the ^{139}La line, δ, even in the absence of the quadrupole interactions and includes chemical, σ, as well as isotropic Knight-shift, K_{iso}, contributions, respectively. The resonance frequency is calculated as $\nu(\theta,\phi) = \nu_L\,[1 + \delta] + \delta\nu_Q(\theta,\phi)$, where angles (θ,ϕ) describe the orientation of the applied magnetic field with respect to the principal-axes system of

EFG tensor and δ is an isotropic NMR shift. Quadrupole effects, which broaden the polycrystalline ^{139}La NMR line, were included up to the second order, $\delta\nu_Q(\theta,\phi) = \delta\nu_Q^{(1)}(\theta,\phi) + \delta\nu_Q^{(2)}(\theta,\phi)$ (see Appendix for details). The characteristic line shape of the central transition immediately suggests that $\eta = 0$, which is also confirmed by the fitting of the central transition polycrystalline line shape [Fig. 2(b)]. This finding is fully compatible with the La residing at the 16*c* position (site symmetry .3.) of the cubic La_2C_3 structure. At room temperature $\nu_Q = 3.10(2)$ MHz is by ≈0.15 MHz smaller compared to the off-stoichiometric La_2C_3 sample with much lower T_c [21]. Therefore, since ^{139}La NMR spectra can be fitted with a single well-defined value of ν_Q, we can rule out significant variations in the carbon stoichiometry of the studied sample. Nevertheless, the absence of sharp singularities for the satellite transitions are accounted for by the small distribution of quadrupole splitting frequencies, $\Delta\nu_Q = 0.16$ MHz, which implies some residual local structural disorder. Excellent matching between the calculated and the measured spectrum at 80 K [Fig. 2(a)] confirms that the NMR signal originates solely from La_2C_3. ^{13}C NMR spectrum of La_2C_3 with a shift $^{13}\delta \approx 340$ ppm and a linewidth $^{13}\Delta\nu \approx 70$ ppm at 100 K (*vide infra*) closely resembles ^{13}C spectrum of the isostructural Y_2C_3 ($^{13}\delta \approx 320$ ppm and $^{13}\Delta\nu \approx 80$ ppm) [18] and has at this temperature an almost identical ^{13}C spin-lattice relaxation time, i.e., $^{13}T_1 = 2.5(10)$ s for La_2C_3 and $^{13}T_1 = 2.6$ s for Y_2C_3 [18]. All these observations unambiguously prove that the measured spectra cannot be attributed to some impurity phase.

^{139}La NMR central transition line [Fig. 2(b)] does not change significantly between 300 and 12 K and can be accounted for at all temperatures by the axially symmetric quadrupole interaction ($\eta = 0$) and weakly temperature dependent ν_Q [Fig. 2(d)]. We conclude that the La site symmetry has not changed in this temperature range, thus implying at the same time the absence of any structural phase transition. The temperature dependence of δ, which is directly related to the local spin susceptibility, χ, through the Knight shift, $K_{iso} = \frac{a_s}{N_A\mu_0}\chi$ (here a_s is a hyperfine constant, N_A is Avogadro's number, and μ_0 is the magnetic permeability of vacuum), is shown in Fig. 2(c). The value of $\delta =$ 3000(50) ppm at room temperature is slightly reduced on cooling and reaches 2890(50) ppm just above T_c. However, a_s is not known *a priori* and thus in order to quantitatively evaluate K_{iso} we use spin-lattice relaxation data next.

In the metallic systems, the Knight shift is directly related to the ^{139}La spin-lattice relaxation time, $^{139}T_1$ through the Korringa relation

$$K_{iso}^2\,{}^{139}T_1T = \frac{\hbar\gamma_e^2}{4\pi k_B\gamma_{139}^2}. \quad (1)$$

Here k_B is Boltzmann constant and γ_e and γ_{139} are the electronic and ^{139}La gyromagnetic ratios, respectively. We neglect the Korringa enhancement factor, because La_2C_3 is believed to be far from any magnetic instability. The temperature dependence of spin-lattice relaxation rate divided by temperature $1/^{139}T_1T$, measured at the high-frequency singularity of the central transition, is shown in Fig. 3(a). $1/^{139}T_1T$ is in the normal state nearly constant, which is compatible with the above-mentioned Korringa relation and weakly temperature-dependent K_{iso}. Inserting the average value $1/^{139}T_1T = 0.192$ s^{-1}K^{-1} into Eq. (1) we calculate $K_{iso} = 1590$ ppm. It is well known for ^{139}La NMR that chemical shifts can be large, even in the several hundred ppm range [27]. Therefore, K_{iso} and σ can explain a significant part, but not the entire magnitude of δ shown in Fig. 2(c).

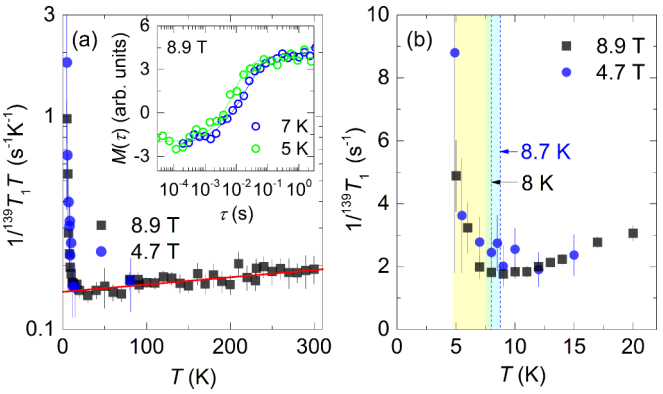

FIG. 3. (Color online) (a) Temperature dependence of ^{139}La spin-lattice relaxation rate $1/^{139}T_1$ divided by temperature measured at the magnetic field of 8.9 T (black solid squares) and 4.7 T (blue solid circles), respectively. A solid line is a guide to the eye indicating a gradual suppression of $1/^{139}T_1T$ with temperature. Inset: comparison of ^{139}La magnetization recovery curves measured at 8.9 T in the superconducting state at 7 (blue circles) and 5 K (green circles) demonstrating the enhanced relaxation rate at lower temperature. (b) Low-temperature dependence of $1/^{139}T_1$ at 8.9 T (black solid squares) and 4.7 T (blue solid circles). Vertical dashed lines indicate expected T_c for 8.9 T (black) and 4.7 T (blue). Light yellow and light blue areas indicate range between T_{c2} and T_c for 8.9 and 4.7 T magnetic field, respectively.

In La_2C_3 multiorbital effects and spin-orbit interactions could give rise to the Van Vleck-like spin susceptibility χ_{VV} [28,29]. The total spin susceptibility, which in the normal state includes Pauli, χ_P, and Van Vleck contributions $\chi = \chi_P + \chi_{VV}$, can thus be strongly enhanced and can account for large δ in the normal state. We note that between 300 and 50 K δ gradually decreases for about 5% [Fig. 2(d)] and that a similar decrease is observed also for $1/^{139}T_1T$. The slight decrease in δ and $1/^{139}T_1T$ with deceasing temperature is probably due to the weakly temperature-dependent χ_P. The decrease of χ_P on cooling—and thus also the related density of states at the Fermi level—may reflect the gradual disappearance of one of the split Fermi surfaces as proposed in Ref. [29].

C. NMR in the superconducting state

Suppression of ^{139}La NMR signal below ≈8 K [Fig. 2(b)] coincides with T_c(8.9 T) deduced from χ_{ac} [Fig. 1(d)]. In the superconducting state the NMR signal intensity decreases because the sample volume, which is penetrated by the rf field, shrinks due to occurrence of supercurrents and thus additionally support the presence of bulk superconductivity in the studied sample.

On cooling below T_c, ^{139}La NMR spectra show down to 4 K no pronounced shift and there is no corresponding suppression of δ from its normal state value, as is typically observed in

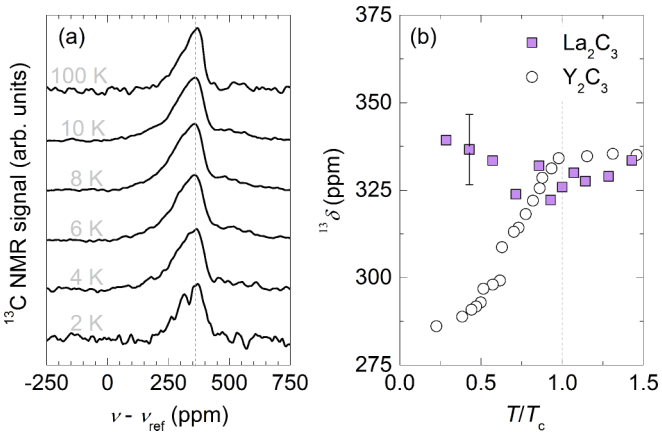

FIG. 4. (Color online) (a) ^{13}C NMR spectrum of polycrystalline La_2C_3 (thick black line) at selected temperatures above and below the critical temperature $T_c(9.39\,T) \approx 7$ K. Vertical dashed line is a guide to the eye indicating that the ^{13}C NMR spectra do not shift below T_c. (b) Temperature dependence of the ^{13}C NMR shift calculated from the first moment of measured spectra (light violet squares). For comparison Y_2C_3 NMR shift data points are included as empty black circles (data was adapted from Harada *et al.* [18]). Vertical dashed line marks $T = T_c$.

superconductors. The temperature independence of K_{iso}—and thus also of local spin susceptibility χ—is surprising and, at a first glance, conflicts with the onset of bulk superconductivity argued above.

To verify that temperature independent NMR shift below T_c is not a peculiar property of ^{139}La nucleus we performed additional ^{13}C NMR measurements in the vicinity of T_c. Similarly to ^{139}La NMR, ^{13}C NMR spectra show no pronounced change on cooling below T_c [Fig. 4(a)] as ^{13}C NMR shift is also nearly temperature independent [$^{13}\delta = 325(10)$ ppm] in the superconducting phase [Fig. 4(b)]. This is in marked contrast to Y_2C_3 ^{13}C NMR measurements where the suppression in the NMR shift for $\Delta\delta \approx 50$ ppm was observed below T_c [18]. The NMR shift due to the vanishing spin susceptibility of pure spin-singlet superconducting state is thus clearly not observed in ^{13}C NMR spectra down to 2 K, in full agreement with ^{139}La NMR data.

We thus finally resort to the measurements of the spin-lattice relaxation time $^{139}T_1$ for $T < T_c$. Measurements of spin-lattice relaxation times have been in the past frequently employed to investigate the symmetry of the superconducting order parameters as very distinct response is observed for isotropic or nodal superconducting gaps [22]. In spin-singlet superconductors $1/T_1$ is exponentially suppressed below T_c due to the opening of the superconducting gap. On the other hand, for nodal superconductors a power-law dependence $1/T_1 \propto T^n$ (with $n \approx 3$) is typically observed [30]. In striking contrast with these expectations, in La_2C_3 $1/^{139}T_1$ increases with decreasing temperature below T_c [inset to Fig. 3(a) and Fig. 3(b)]. The enhancement of $1/^{139}T_1$ is very strong and continues to monotonically increase down to $0.63T_c$ so that it cannot be attributed simply to the Hebel-Slichter coherence peak of a conventional s-wave superconductor. Such temperature dependence is in marked contrast to ^{13}C spin-lattice measurements in the isostructural Y_2C_3 where $1/^{13}T_1$ exponentially drops below T_c showing multigap behavior without any signature of the Hebel-Slichter coherence peak [18] or to the off-stoichiometric La_2C_3 sample with suppressed T_c where the Hebel-Slichter coherence peak has been followed by an exponential decay of spin-lattice relaxation time in agreement with the conventional s-wave superconductivity [21]. To search for a suppression of spin-lattice relaxation rate below T_c additional $^{139}T_1$ measurements were performed at a lower field of 4.7 T where $T_c = 8.7$ K and $T_{c2} = 7.5$ K are higher [light blue area in Fig. 3(b)]. However, even in this case no characteristic drop in $1/^{139}T_1$ could be observed down to 4.9 K ($\approx 0.56T_c$ at 4.7 T). Therefore, just like δ discussed above, $1/^{139}T_1$ also shows unconventional behavior below T_c.

IV. DISCUSSION

Although different probes employed in this study clearly detect bulk superconductivity below $T_c = 11.8(2)$ K in the present high-quality La_2C_3 polycrystalline sample, there are some striking anomalies that point towards its unconventional nature. The first surprising finding is that NMR shifts are almost insensitive to the superconducting transition at T_c as they remain down to $T \approx 0.25T_c$ nearly constant at their normal-state values of 2890(50) ppm and 325(10) ppm for ^{139}La and ^{13}C NMR spectra, respectively. In a conventional s-wave superconductors spin susceptibility vanishes due to the opening of the superconducting gap and as a result $K_{iso} \to 0$ [22]. Therefore, in the case of ^{139}La NMR a significant suppression of δ by $\sim$1600 ppm is expected, which is not observed in our measurements. Similarly, a shift of ^{13}C NMR spectra by approximately 50 ppm observed in Y_2C_3 [18] is significantly larger than the uncertainty of our measurements on La_2C_3 thus leading to the same conclusion on the temperature independence of Knight shift in the superconducting state. There are only a few superconducting systems that show similarly anomalous behavior in the NMR shift [13,14,28,31]. In Ref. [28] the contribution from χ_{VV}, which does not change on cooling into the superconducting state, has been considered to mask the suppression of spin susceptibility in the superconducting state. However, as argued above, although χ_{VV} is clearly present and important in La_2C_3, it is at the same time not large enough to prevail over the Knight shift and, therefore, it cannot be responsible for the anomalous temperature-independent δ below T_c. Thus, scenario of spin-singlet s-wave superconductivity with the dominant χ_{VV} can be ruled out for the studied La_2C_3 sample. On the other hand, nearly temperature-independent Knight shift below T_c has been also discussed in terms of spin-triplet superconductivity, e.g., in Sr_2RuO_4 [31], UPt_3 [13], or in Li_2Pt_3B [14]. Moreover, strong asymmetric spin-orbit coupling associated with the heavy Pt atoms was proposed to mix spin-singlet and spin-triplet states in Li_2Pt_3B [9,14]. When the pinning interaction that acts on the triplet pairs and locks the spins of a superconducting pair in a certain direction of the crystal is strong, a very anisotropic response is expected for such mixed states [8]. Similarly to Li_2Pt_3B, the noncentrosymmetric structure of La_2C_3 allows for the asymmetric spin-orbit coupling. Therefore, if superconductivity in La_2C_3 has similar origin as in Li_2Pt_3B, then δ of our polycrystalline sample should be at least partially suppressed. Since this is not

the case, the only possible explanation would be that pinning interactions are sufficiently weak so that Cooper-pair spins can reorient easily toward the applied magnetic field making the Knight shift invariant for any field direction.

However, compounds with mixed spin-singlet and spin-triplet states usually still display suppressed spin-lattice relaxation rates below T_c as a result of opening of the (nodal) superconducting gap. In this respect present ^{139}La NMR measurements do not directly classify La_2C_3 into the same category of superconductors. In fact, the temperature dependence of $1/^{139}T_1$ in La_2C_3 is much more reminiscent to some superconducting LiFeAs samples which show both temperature-independent shifts and enhanced spin-lattice relaxation [32,33]. Four different possibilities for the increase in $1/T_1$ in these LiFeAs samples were listed in the literature [33,34]: (i) impurity contributions, (ii) slowing down of magnetic fluctuations due to the opening of the superconducting gap, (iii) vortex-dynamics contributions, or (iv) collective modes of the spin-triplet pairs leading to novel spin dynamics in the superconducting state. Possibility (i) can be directly ruled out in La_2C_3, because no paramagnetic impurity signal was detected in EPR measurements [Fig. 1(c)]. Similarly, possibility (ii) can be discarded since La_2C_3 is far away from any magnetic instability.

In order to discuss possibility (iii) we first stress that the observation of strong MMMA signal [Fig. 1(c)] is compatible with the vortex fluctuations in La_2C_3. We also note that a new type of vortex pinning was proposed in a noncentrosymmetric superconductor leading to the anomalous vortex avalanches [35] that could result in the vortex-dynamics enhancement of spin-lattice relaxation rates below T_c [36–38]. However, so far the vortex-dynamics contributions to spin-lattice relaxation have been detected only in compounds with very small $1/T_1$ [34], i.e., typically in systems with $1/T_1T \sim 10^{-2} - 10^{-4}$ s^{-1}K^{-1}. Therefore, $1/^{139}T_1T$ values [Fig. 3(a)] measured on La_2C_3 seem not to fall into the appropriate spin-lattice relaxation rate window where the vortex-dynamics contribution could become relevant. Moreover, the absence of the characteristic narrowing of ^{13}C spectra and the constant ^{13}C shift are also incompatible with the vortex-dynamics scenario.

Finally, present data does not provide sufficient arguments for or against the exotic spin-triplet modes [possibility (iv)] that would be allowed in La_2C_3 due to the asymmetric spin-orbit coupling thus leaving this possibility wide open. Nevertheless we realize that this remaining option presents a coherent explanation for the temperature-independent δ and the enhancement of $1/^{139}T_1$ in the superconducting state if the mixing of spin-singlet and spin-triplet superconducting pairs occurs in La_2C_3.

V. CONCLUSIONS

In conclusion, the noncentrosymmetric La_2C_3 superconductor was comprehensively investigated with ^{139}La and ^{13}C NMR. Although static and dynamic magnetization measurements and MMMA signal imply bulk superconductivity below $T_c = 11.8$ K, the anomalous ^{139}La NMR shift and spin-lattice relaxation rates indicate an unconventional superconducting state. In particular, the temperature-independent ^{139}La and ^{13}C NMR shifts in the superconducting state can be taken as an evidence for the mixing of spin-singlet and spin-triplet pairs. The large ^{139}La NMR shift partially arises from the Van Vleck-like susceptibility that is attributed to the asymmetric spin-orbit coupling, which then provides a microscopic mechanism for the mixing of singlet and triplet pairs in the superconducting state.

ACKNOWLEDGMENTS

D.A. acknowledges the financial support by the European Union FP7-NMP-2011-EU-Japan project LEMSUPER under Contract No. 283214. Work at AGU is supported by the Strategic International Collaborative Research Program (SICORP-LEMSUPER) from Japan Science and Technology Agency (JST), Grant-in-Aid from Ministry of Education, Culture, Sports, Science and Technology (MEXT) under Grant No. 25000003, and MEXT-Supported Program for the Strategic Research Foundation at Private Universities, 2013-2017. J.A. and D.A. thank Professor Kitaoka and Professor Mukuda of Osaka University for sharing their unpublished data [21].

APPENDIX: SIMULATION OF NMR SPECTRUM

In order to correctly simulate the entire ^{139}La NMR spectrum, quadrupole interaction is considered up to the second order for both the central and the satellite transitions.

The resonant frequency is in general calculated with the following expression

$$\nu(\theta,\phi) = \nu_L[1 + \delta(\theta',\phi')] + \delta\nu_Q^{(1)}(\theta,\phi) + \delta\nu_Q^{(2)}(\theta,\phi), \quad \text{(A1)}$$

where $\delta(\theta',\phi')$ is NMR shift, $\nu_Q^{(i)}(\theta,\phi)$ is quadrupole shift in the ith order, θ' and ϕ' are polar and azimuthal angles of the magnetic field orientation with respect to the NMR shift tensor, and θ and ϕ are polar and azimuthal angles with respect to the quadrupole tensor principal axes.

The NMR shift tensor $(\delta_{i,j})$ is expressed as [25]:

$$\delta(\theta',\phi') = \delta_{\text{iso}} + \delta_{\text{ani}}\frac{3\cos^2\theta' - 1}{2} + \delta_{\text{asy}}\sin^2\theta'\cos 2\phi', \quad \text{(A2)}$$

where $\delta_{\text{iso}} = (\delta_{xx} + \delta_{yy} + \delta_{zz})/3$, $\delta_{\text{ani}} = (2\delta_{zz} - \delta_{xx} - \delta_{yy})/3$, and $\delta_{\text{asy}} = (\delta_{xx} - \delta_{yy})/2$.

The quadrupole shift in the ith order is expressed as follows [25,39]:

$$\nu_Q^{(i)}(\theta,\phi) = \frac{1}{h}\sum_{m=-I}^{I-1} E^{(i)}(I,m,\theta,\phi) - E^{(i)}(I,m-1,\theta,\phi), \quad \text{(A3)}$$

where I is the nuclear spin number and m is the nuclear spin projection on the quantization axes. The first- and the

second-order quadrupole energy contributions are

$$E^{(1)}(I,m) = \frac{h\nu_Q}{4}\left(m^2 - \frac{I(I+1)}{3}\right)(3\cos^2\theta - 1 + \eta\sin\theta^2\cos 2\phi), \tag{A4}$$

$$E^{(2)}(I,m) = \frac{1}{18}\frac{h\nu_Q^2}{\nu_L}m(T_1 + T_2 + T_3),$$

$$T_1 = -\frac{1}{5}(I(I+1) - 3m^2)(\eta^2 + 3),$$

$$T_2 = \frac{1}{28}(8I(I+1) - 12m^2 - 3)((\eta^2 - 3)(3\cos^2\theta - 1) + 6\eta\sin^2\theta\cos 2\phi), \tag{A5}$$

$$T_3 = \frac{1}{8}(18I(I+1) - 34m^2 - 5)$$
$$\times\left(\frac{1}{140}(\eta^2 + 18)(35\cos^4\theta - 30\cos^2\theta + 3) + \frac{3}{7}\eta\sin^2\theta(7\cos^2\theta - 1)\cos 2\phi + \frac{1}{4}\eta^2\sin^4\theta(2\cos^2 2\phi - 1)\right).$$

The NMR spectrum is computed as a histogram of resonance frequencies Eq. (A1) obtained with uniformly distributed $\cos\theta'$, ϕ', $\cos\theta$, and ϕ and convoluted with a Gaussian function simulating homogeneous broadening. The quadrupole resonance transition frequencies between m and $m-1$ states are in the histogram weighted as

$$w_{m,m-1} = I(I+1) - m(m-1). \tag{A6}$$

For the simulation of quadrupole splitting frequency distribution the spectra are calculated using normally distributed values with the center at ν_Q and width of $\Delta\nu_Q$.

[1] D. Arčon, K. Anderle, M. Klanjšek, A. Sans, C. Mühle, P. Adler, W. Schnelle, M. Jansen, and C. Felser, Phys. Rev. B **88**, 224409 (2013).

[2] S. Riyadi, B. Zhang, R. A. de Groot, A. Caretta, P. H. M. van Loosdrecht, T. T. M. Palstra, and G. R. Blake, Phys. Rev. Lett. **108**, 217206 (2012).

[3] Y. Takabayashi, A. Y. Ganin, P. Jeglič, D. Arčon, T. Takano, Y. Iwasa, Y. Ohishi, M. Takata, N. Takeshita, K. Prassides *et al.*, Science **323**, 1585 (2009).

[4] A. Y. Ganin, Y. Takabayashi, P. Jeglič, D. Arčon, A. Potočnik, P. J. Baker, Y. Ohishi, M. T. McDonald, M. D. Tzirakis, A. McLennan *et al.*, Nature (London) **466**, 221 (2010).

[5] G. Amano, S. Akutagawa, T. Muranaka, Y. Zenitani, and J. Akimitsu, J. Phys. Soc. Jpn. **73**, 530 (2004).

[6] X. Wang, I. Loa, K. Syassen, R. K. Kremer, A. Simon, M. Hanfland, and K. Ahn, Phys. Rev. B **72**, 064520 (2005).

[7] S. Fujimoto, J. Phys. Soc. Jpn. **76**, 051008 (2007).

[8] L. P. Gor'kov and E. I. Rashba, Phys. Rev. Lett. **87**, 037004 (2001).

[9] H. Q. Yuan, D. F. Agterberg, N. Hayashi, P. Badica, D. Vandervelde, K. Togano, M. Sigrist, and M. B. Salamon, Phys. Rev. Lett. **97**, 017006 (2006).

[10] E. Bauer, G. Hilscher, H. Michor, C. Paul, E. W. Scheidt, A. Gribanov, Y. Seropegin, H. Noël, M. Sigrist, and P. Rogl, Phys. Rev. Lett. **92**, 027003 (2004).

[11] T. Akazawa, H. Hidaka, T. Fujiwara, T. C. Kobayashi, E. Yamamoto, Y. Haga, R. Settai, and Y. Onuki, J. Phys.: Condens. Matter **16**, L29 (2004).

[12] N. Tateiwa, Y. Haga, T. D. Matsuda, S. Ikeda, E. Yamamoto, Y. Okuda, Y. Miyauchi, R. Settai, and Y. Onuki, J. Phys. Soc. Jpn. **76**, 083706 (2007).

[13] H. Tou, Y. Kitaoka, K. Ishida, K. Asayama, N. Kimura, Y. Onuki, E. Yamamoto, Y. Haga, and K. Maezawa, Phys. Rev. Lett. **80**, 3129 (1998).

[14] M. Nishiyama, Y. Inada, and G.-q. Zheng, Phys. Rev. Lett. **98**, 047002 (2007).

[15] J. Chen, M. B. Salamon, S. Akutagawa, J. Akimitsu, J. Singleton, J. L. Zhang, L. Jiao, and H. Q. Yuan, Phys. Rev. B **83**, 144529 (2011).

[16] J. S. Kim, W. Xie, R. K. Kremer, V. Babizhetskyy, O. Jepsen, A. Simon, K. S. Ahn, B. Raquet, H. Rakoto, J.-M. Broto *et al.*, Phys. Rev. B **76**, 014516 (2007).

[17] S. Kuroiwa, Y. Saura, J. Akimitsu, M. Hiraishi, M. Miyazaki, K. H. Satoh, S. Takeshita, and R. Kadono, Phys. Rev. Lett. **100**, 097002 (2008).

[18] A. Harada, S. Akutagawa, Y. Miyamichi, H. Mukuda, Y. Kitaoka, and J. Akimitsu, J. Phys. Soc. Jpn. **76**, 023704 (2007).

[19] A. L. Giorgi, E. G. Szklarz, M. C. Krupka, and N. H. Krikorian, J. Less-Common Met. **17**, 121 (1969).

[20] J. S. Kim, R. K. Kremer, O. Jepsen, and A. Simon, Curr. Appl. Phys. **6**, 897 (2006).

[21] Y. Kitaoka and H. Mukuda (unpublished).

[22] R. E. Walstedt, *The NMR Probe of High-Tc Materials* (Springer, Berlin, 2008).

[23] T. Shaposhnikova, Y. Talanov, and Y. Vashakidze, Physica C: Superconductivity **385**, 383 (2003).

[24] N. Y. Panarina, Y. I. Talanov, T. S. Shaposhnikova, N. R. Beysengulov, E. Vavilova, G. Behr, A. Kondrat, C. Hess, N. Leps, S. Wurmehl *et al.*, Phys. Rev. B **81**, 224509 (2010).

[25] A. Abragam, *Principles of Nuclear Magnetism* (Oxford University Press, Oxford, 1986).

[26] A. Suter, M. Mali, J. Roos, and D. Brinkmann, J. Phys.: Condens. Matter **10**, 5977 (1998).
[27] S. Leyer, S. Heck, A. Kaiser, E. Dormann, and R. G. Barnes, Phys. Rev. B **72**, 125115 (2005).
[28] M. Udagawa and Y. Yanase, J. Phys. Soc. Jpn. **79**, 123601 (2010).
[29] D. Maruyama and Y. Yanase, J. Phys. Soc. Jpn. **82**, 084704 (2013).
[30] T. Imai, T. Shimizu, H. Yasuoka, Y. Ueda, and K. Kosuge, J. Phys. Soc. Jpn. **57**, 2280 (1988).
[31] K. Ishida, H. Mukuda, Y. Kitaoka, K. Asayama, Z. Q. Mao, Y. Mori, and Y. Maeno, Nature (London) **396**, 658 (1998).
[32] S.-H. Baek, H.-J. Grafe, F. Hammerath, M. Fuchs, C. Rudisch, L. Harnagea, S. Aswartham, S. Wurmehl, J. v. d. Brink, and B. Büchner, Eur. Phys. J. B **85**, 159 (2012).
[33] S.-H. Baek, L. Harnagea, S. Wurmehl, B. Büchner, and H.-J. Grafe, J. Phys.: Condens. Matter **25**, 162204 (2013).
[34] Y. Nakai, K. Ishida, Y. Kamihara, M. Hirano, and H. Hosono, Phys. Rev. Lett. **101**, 077006 (2008).
[35] C. F. Miclea, A. C. Mota, M. Sigrist, F. Steglich, T. A. Sayles, B. J. Taylor, C. A. McElroy, and M. B. Maple, Phys. Rev. B **80**, 132502 (2009).
[36] L. Bossoni, P. Carretta, A. Thaler, and P. C. Canfield, Phys. Rev. B **85**, 104525 (2012).
[37] L. Bossoni, P. Carretta, W. P. Halperin, S. Oh, A. Reyes, P. Kuhns, and P. C. Canfield, Phys. Rev. B **88**, 100503 (2013).
[38] L. Bossoni, P. Carretta, M. Horvatić, M. Corti, A. Thaler, and P. C. Canfield, Europhys. Lett. **102**, 17005 (2013).
[39] M. J. Duer, *Solid State NMR Spectroscopy: Principles and Applications* (Wiley, New York, 2008).